



Research Article

Combustion Synthesis of Al_2O_3 Ceramic Powders

S. M. Rafiaei *¹*Materials Engineering Group, Golpayegan College of Engineering, Isfahan University of Technology, Golpayegan, Iran.*

ARTICLE INFO

Keywords:

Combustion Synthesis, Aluminum Nitrate, Aluminum Acetate, Nanostructure, Refractories.

Article history:

Received 04 April 2024

Received in revised form 02 Jun 2024

Accepted 06 August 2024

ABSTRACT

In this research, Al_2O_3 powders were successfully synthesized by employing different initial materials of aluminum nitrate and aluminum acetate through the facile solution combustion approach. Al_2O_3 based insulation materials possess many essential applications in steel manufacturing industries regarding their considerable heat-resistance characteristics. To study the crystal structure, microstructure, and surface chemistry of the synthesized oxides, X-ray diffraction (XRD), scanning electron microscope (SEM), and Fourier transform infrared spectroscopy (FTIR) were employed. It was found that the use of aluminum acetate facilitates the synthesis of semi-crystalline Al_2O_3 in the synthesis condition, while regardless of the used initial materials, calcination treatment at 1000 °C gives rise to the improvement of crystallinity. Additionally, the SEM observations clarified that through the employment of aluminum acetate, very fine particles with the approximate size of 1 μm were produced. The FTIR characterizations revealed that the peaks at 570 and 790 cm^{-1} originate from Al-O bonds in the octahedral and tetrahedral coordination and confirmed the synthesis of Al_2O_3 . In short, to produce Al_2O_3 powders, the utilization of combustion by urea fuel and aluminum acetate brings appropriate characterizations.

1. Introduction

Nowadays, there are many industries like steel manufacturing that use vast amounts of refractory materials. Recent urgent needs for controlled energy usage and adequate energy consumption require high-quality thermal insulation compounds. The research in the fields of refractory compounds addresses the mentioned demands.

Although traditional refractory bricks used in steel manufacturing possess sue heat-resistance applications and their final cost is relatively low, they are now being substituted by advanced insulators such as alumina wool and mullite wool. However, if the conventional cheap refractory compounds can be produced in porous shapes, their performance and insulation characteristics at elevated temperatures will be improved. Herein, the porous refractory bricks can be considered a proper candidate for many vital industries. Now, many ceramics such as alumina, silica and spinels can be employed as refractory ceramics [1-7]. Al_2O_3 is one of the common oxides used in different applications [8]. Alumina-based materials, such as α/β alumina, a mixture of α/β alumina and mullite ($Al_6Si_2O_{13}$), provide suitable alternatives to silicon oxide [9]. In addition, alumina can be synthesized through different approaches like solid state, Sol-Gel, combustion and ets. [10-11]. Different synthesis approaches bring

**Corresponding author*Email: s.rafiaei@iut.ac.ir

Address: Materials Engineering Group, Golpayegan College of Engineering, Isfahan University of Technology, Golpayegan, Iran

1. Associate Professor

DOI: <http://10.22034/IJISSI.2024.2025939.1284>

Published by ISSI (Iron & Steel Society of Iran)

versatile characterizations suitable for various applications [12-13]. In this research combustion synthesis was employed since it can provide fine and uniform particle size [14-17]. In addition, given that for the insulation properties, the synthesized alumina should be porous, one can expect that combustion synthesis can be considered as excellent approach for the production of alumina. Meanwhile, this approach is speedy and low amounts of energy is consumed. In other words, the main benefits of facile combustion synthesis are the relatively low cost of equipment, low ignition temperature, production of porous materials, and proper homogeneity of products. Additionally, this approach is also considered as an economic technique because an exothermic reaction results in production of remarkable amounts of heat within a short period as well as generation a porous nanostructure [18-20].

Motivated by this background, to synthesis alumina, combustion method was carried out by the utilization of aluminum nitrate and aluminum acetate, individually. Meanwhile, the crystal structure, microstructure, and surface chemistry of the synthesized alumina powders were characterized by X-ray diffraction (XRD), scanning electron microscope (SEM), and Fourier transform infrared spectroscopy (FTIR).

2. Experimental

2.1. Materials Preparation

The combustion synthesis method was considered to produce Al_2O_3 ceramic powders. The starting materials including aluminum nitrate ($\text{Al}(\text{NO}_3)_3 \cdot 6\text{H}_2\text{O}$), aluminum acetate ($\text{Al}(\text{CH}_3\text{COO})_3$), and urea ($\text{CH}_4\text{N}_2\text{O}$) were purchased at the highest possible grade. In a typical synthesis of Al_2O_3 nano-ceramics, aluminum nitrate and or aluminum acetate was dissolved in a very small amount of de-ionized water and gently stirred for 15 minutes at the ambient temperature in an alumina crucible. Then, urea was added to the mixture during vigorous stirring. The obtained precursor solution was transferred into an electric furnace at $500\text{ }^\circ\text{C}$ (see Fig. 1). The spontaneous combustion leads to making foamy and low dense production in the crucible. To remove the remaining organic

compounds and suitable crystallinity, the powders were heated at the temperature of $1000\text{ }^\circ\text{C}$ for two h. The temperature of $1000\text{ }^\circ\text{C}$ is an optimum temperature for getting crystallized Al_2O_3 since higher temperatures leads to sever growth of particles and waste of energy. It should be noted that the explained procedure was carried out by both of aluminum nitrate and aluminum acetate, individually.

2.2. Materials Characterization

The crystal structures of our materials were characterized by X-ray diffraction (XRD, Rigaku, Japan) with a rotating anode and $\text{Cu K}\alpha$ radiation source ($\lambda = 0.15418\text{ nm}$). To draw the crystal structure of alumina, VESTA software was utilized. In addition, to study the microstructure of ceramics, a scanning electron microscope (SEM, JSM6360, Japan) was employed. Meanwhile, Fourier transform infrared spectroscopy (FT-IR, Thermo Science Nicolet 6700, USA) was used to study the surface chemistry of the synthesized oxide.

3. Results and discussion

3.1. Thermodynamics and Crystallography

As it was already explained, the used initial materials for the combustion synthesis can be $\text{Al}(\text{NO}_3)_3 \cdot 6\text{H}_2\text{O}$ / $\text{Al}(\text{CH}_3\text{COO})_3$ and $\text{CH}_4\text{N}_2\text{O}$. Given that the exist water molecules in $\text{Al}(\text{NO}_3)_3 \cdot 6\text{H}_2\text{O}$ will be evaporated within the combustion process, one can expect that $\text{Al}(\text{NO}_3)_3$ can be considered as the initial material in the related reaction.

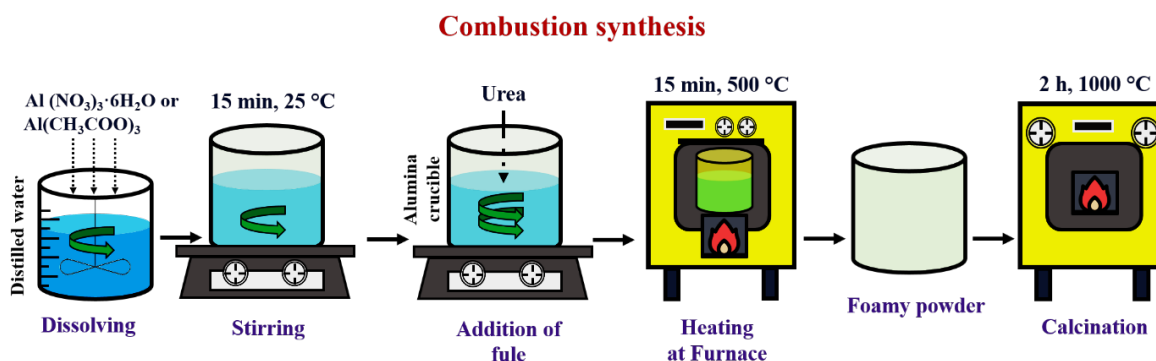
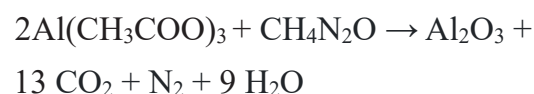
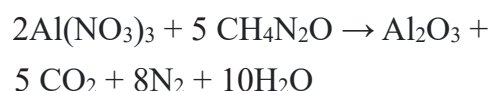


Fig. 1. Schematic view of combustion synthesis of Al_2O_3 nanoparticles.

Accordingly, it is seen that via the production of 1 mol Al_2O_3 , large amounts of gaseous molecules (23 mol) are released. This phenomenon results in the production of porous and fine particles of Al_2O_3 . Meanwhile, it can be easily found that the employed combustion procedure can be known as a green approach since the released gases are not dangerous components for our environment. The produced temperature (T_f) in the mentioned combustion synthesis can be easily estimated as follows:

$$T_f = T_0 + (\Delta H_r - \Delta H_p)/C_p \quad \text{Eq.(3)}$$

Where T_0 is the initial temperature that, as was described earlier, in this work is 500 °C. Additionally, ΔH_r , ΔH_p , and C_p are formation enthalpies of reactants,

formation enthalpies of products, and heat capacity of products at the constant pressure, respectively. Shokouhimehr et al. showed that the obtained T_f of the combustion synthesis can approximately reach the high temperature of 2200 °C [4]. Fig. 2. shows the molecular structure of $\text{CH}_4\text{N}_2\text{O}$ and also the crystal Structure of Al_2O_3 . Correspondingly, the CIF 1008776 and 1000017 were used, respectively. The molecular structure of $\text{CH}_4\text{N}_2\text{O}$ possesses a short range ordering while that of Al_2O_3 shows a well ordered and crystallized structure with a space group of Fm-3m. Tables 1 and 2. show the crystallographic characterizations of $\text{CH}_4\text{N}_2\text{O}$ and Al_2O_3 , respectively. Herein, the atomic coordinates, space groups, unit-cell volumes, lattice parameters, and lattice angles have been presented.

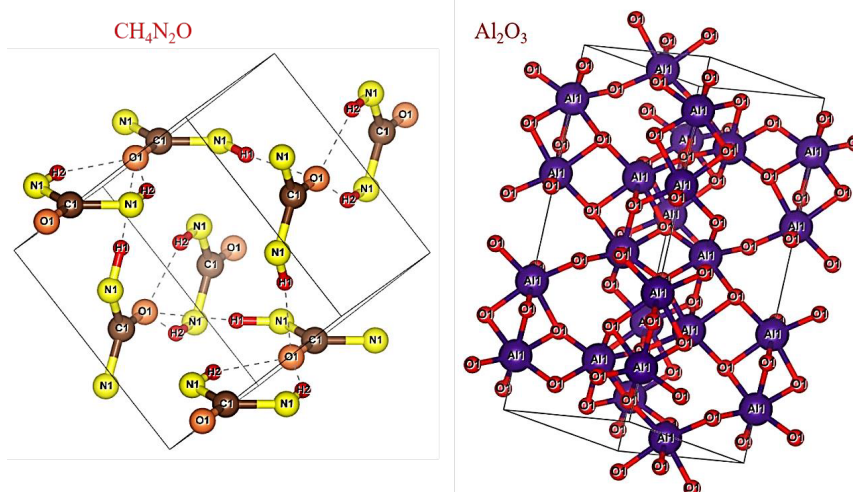


Fig. 2. Crystal Structures of $\text{CH}_4\text{N}_2\text{O}$ and Al_2O_3 .

Table 1. Crystallographic characterizations of $\text{CH}_4\text{N}_2\text{O}$.

Formula		x	y	z	Space group name	Space group number	Unit-cell volume
$\text{CH}_4\text{N}_2\text{O}$	1 C	0.00000	0.50000	0.33300	P -4 21 m	113	151.005076 Å ³
	2 O	0.00000	0.50000	0.59680	a	B	c
	3 N	0.14390	0.64390	0.18320	5.66100	5.66100	4.71200
	4 H	0.25220	0.75220	0.28390	alpha	Beta	gamma
	5 H	0.13650	0.63650	0.97240	90.00	90.00	90.00

Table 2. Crystallographic characterizations of Al_2O_3 .

Formula		x	y	z	Space group name	Space group number	Unit-cell volume
Al_2O_3	1 O	0.69365	0.00000	0.25000	R -3 c	167	255.033311 Å ³
	2 Al	0.00000	0.00000	0.35217	a	B	c
					4.76060	4.76060	12.99400
					alpha	Beta	gamma
				90.00	90.00	120.00	

3.2. Crystal Structure

Fig. 3. shows the X-ray diffraction (XRD) spectrum for the combustion synthesized Al_2O_3 powders, when aluminum nitrate ($\text{Al}(\text{NO}_3)_3 \cdot 6\text{H}_2\text{O}$) was used as the initial material. It is seen that after synthesis, the production possesses an amorphous structure. In other words, the combustion temperature was not enough to eliminate the organic compounds of the used fuel. So, the powders were calcined at 1000°C for 2 h. The related XRD spectrum reveals that the crystal structure of the calcined alumina powder has formed successfully. It has been shown that the XRD spectrum is in a good fitting with JCPDS No. 01-075-0921. Similarly, Fig. 4. shows the XRD spectrum for the combustion synthesized Al_2O_3 powders, when aluminum citrate ($\text{Al}(\text{CH}_3\text{COO})_3$) was used as the initial material. It is seen that the XRD graph of the calcined oxide agrees well with JCPDS No. 00-001-1303. It is observed that after 2 h of calcination at 1000°C the XRD spectrum has dramatically changed from semi crystalline to fully crystalline situation. In other words, the temperature of 1000°C has been very effective for evaporating the organic compounds and improving the crystallinity of productions. The crystallographic characterizations of the synthesized Al_2O_3 using aluminum nitrate and aluminum citrate have been compared in Table 3. Interestingly, the use of mentioned

initial materials leads to very similar crystallographic characterizations but the use of aluminum citrate gives rise to the formation of more proper chemical formula of Al_2O_3 production with a smaller unit cell volume.

3.3. Microstructure Observations

Fig. 5. shows the SEM images of combustion synthesized Al_2O_3 powders after calcination at 1000°C when aluminum nitrate ($\text{Al}(\text{NO}_3)_3 \cdot 6\text{H}_2\text{O}$) was used as the initial material. It is found that the particle size is mainly in the range of 1-4 μm while severe aggregation has occurred.

Fig. 6. shows the SEM images of Al_2O_3 powders after calcinations at 1000°C . when aluminum acetate ($\text{Al}(\text{CH}_3\text{COO})_3$) was used as the raw material. In this condition, the approximate particle size is 1 μm and almost no aggregation can be seen. Noteworthy, through the use of $\text{Al}(\text{CH}_3\text{COO})_3$, the particle sizes of the production are in a very narrow distribution.

3.4. FTIR Analysis

Fig. 7. presents the FTIR images of the combustion synthesized Al_2O_3 powders by the use of aluminum nitrate ($\text{Al}(\text{NO}_3)_3 \cdot 6\text{H}_2\text{O}$) and aluminum acetate ($\text{Al}(\text{CH}_3\text{COO})_3$).

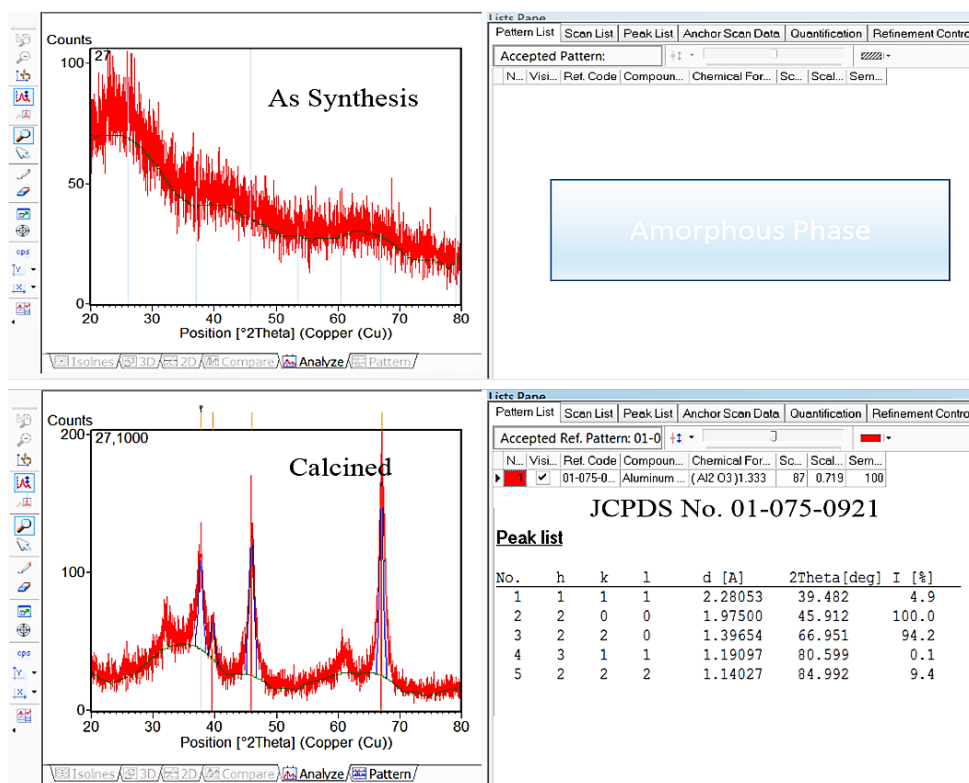


Fig. 3. XRD spectra of the combustion synthesized Al_2O_3 powders (using aluminum nitrate).

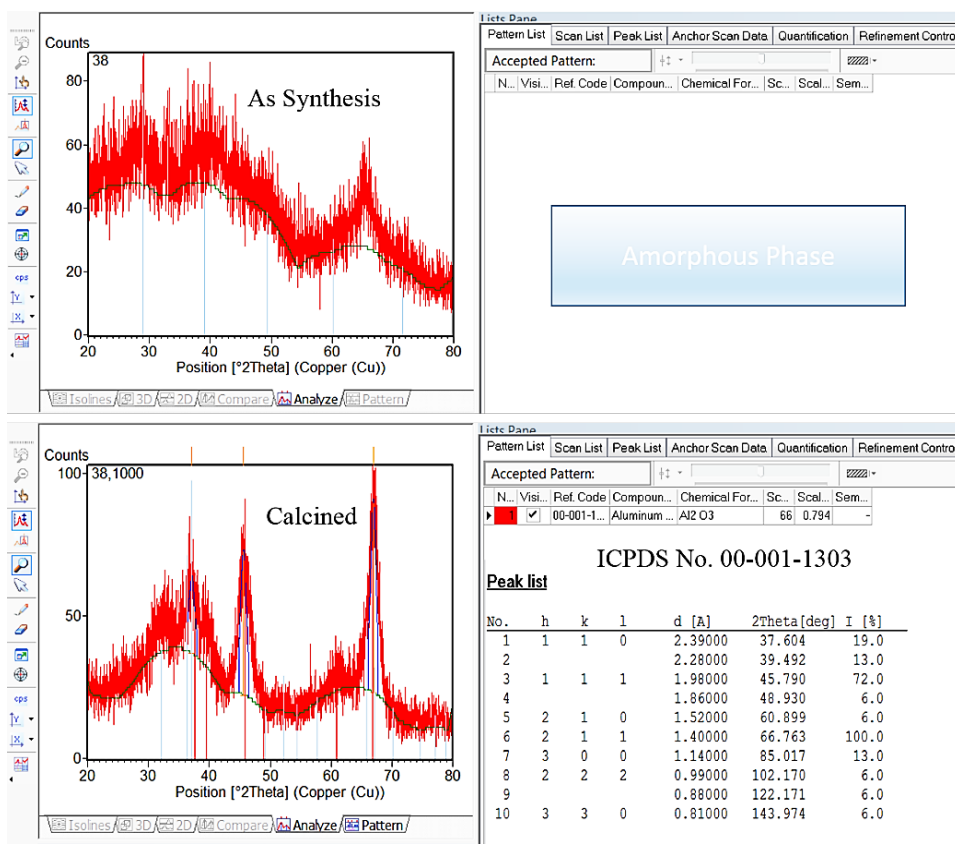


Fig. 4. XRD spectra of the combustion synthesized Al₂O₃ powders (using aluminum citrate).

Table 3. Crystallographic characterizations of Al₂O₃ synthesized by the use of Aluminum nitrate/citrate.

Items	Aluminum Nitrate	Aluminum Citrate
Reference Code	01-075-0921	00-001-1303
ICSD Name	Aluminum Oxide	Aluminum Oxide
Empirical Formula	Al _{2.666} O _{3.999}	Al ₂ O ₃
Chemical Formula	(Al ₂ O ₃) _{1.333}	Al ₂ O ₃
Crystal System	Cubic	Cubic
Space Group	Fm-3m	Fm-3m
Space Group No.	225	225
a (Å)	3.95	3.41
b (Å)	3.95	3.41
c (Å)	3.95	3.41
Alpha (°)	90	90
Beta (°)	90	90
Gamma (°)	90	90
Calculated Density (g/cm ³)	3.66	3.47
Volume of Cell (10 ⁶ pm ³)	61.63	39.65

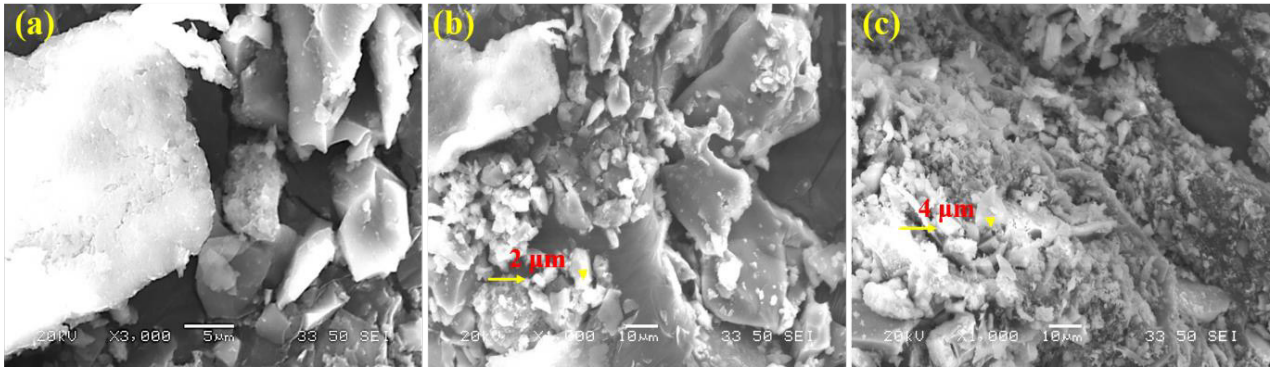


Fig. 5. SEM images of combustion synthesized Al₂O₃ powders (by the use of aluminum nitrate (Al(NO₃)₃·6H₂O)).

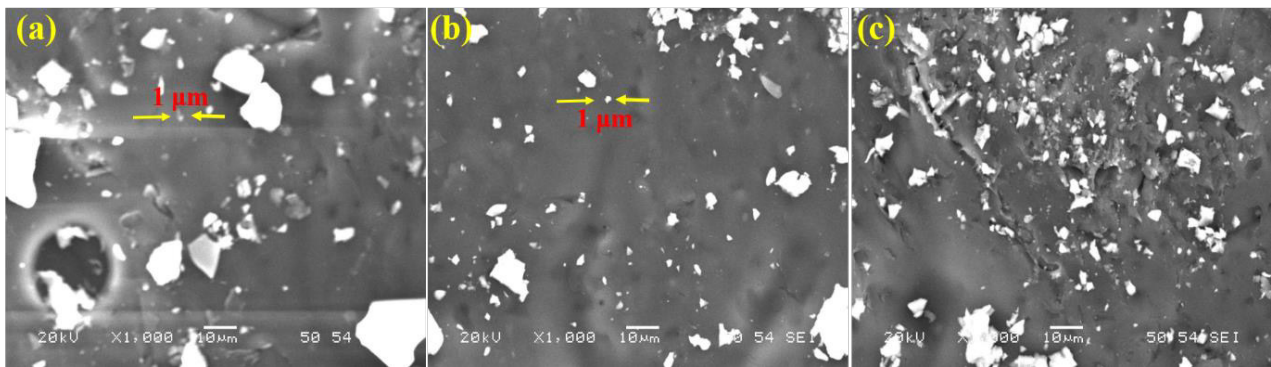


Fig. 6. SEM images of combustion synthesized Al₂O₃ powders (by the use of aluminum acetate (Al(CH₃COO)₃)).

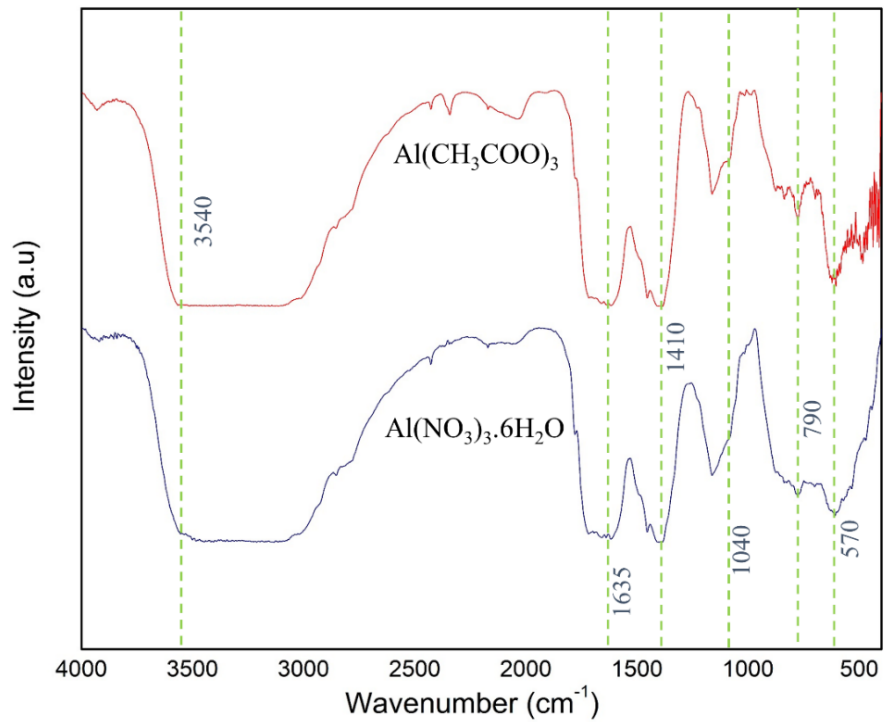


Fig. 7. The FTIR images of the combustion synthesized Al₂O₃ powders by the use of aluminum nitrate (Al(NO₃)₃·6H₂O) and aluminum acetate (Al(CH₃COO)₃).

Correspondingly, the very weak peaks at 570 and 790 cm^{-1} are attributed to Al-O bonds in the octahedral and tetrahedral coordination. The formation of this bond interestingly confirms the successful synthesis of Al_2O_3 insulation materials. Additionally, the slight band at 1040 cm^{-1} is attributed to Al-O-H bonds. Herein, this band is attributed to the bonding between Al_2O_3 and the surface moisture and hydroxyl groups. The literature survey reveals that the band appearing at about 1410 cm^{-1} originates from the presence of CO_3^{2-} groups. Furthermore, the infrared absorption peaks at 1634 and 3540 cm^{-1} arises from the surface moisture and the stretching vibration of O-H bond [12-13].

4. Conclusions

In this paper, Al_2O_3 powders were successfully synthesized by employing different initial materials via a combustion approach. The XRD analysis revealed that although both aluminum nitrate and aluminum acetate provide the production of crystallized Al_2O_3 (after calcination) while the use of aluminum acetate facilitates the synthesis of Al_2O_3 crystal structure with smaller crystallite size and crystal volume. Moreover, the SEM observations proved that the employment of aluminum acetate leads to the formation of very fine microstructure with the approximate particle size of 1 μm while no severe aggregation was occurred. Furthermore, FTIR analysis confirmed the successful syntheses of Al_2O_3 .

References

- [1] Singh V, Chakradhar R.P.S, Rao J.L, Kim D.K, Combustion synthesized MgAl_2O_4 : Cr phosphors An EPR and optical study, *J. Lumin.* 2009; 129: 130.
- [2] Rafiaei S.M, Ashrafi F, et al. Enhanced luminescence properties of phosphors coated by silica nano-layers: Study of reflection and emission, *Ceramics International.* 2019; 45: 1670-1675.
- [3] Rafiaei S.M, Shokouhimehr M, Impact of process parameters on luminescence properties and nanostructure of YVO_4 :Eu phosphor, *Materials Chemistry and Physics.* 2019; 229: 431-436.
- [4] Rafiaei S.M, Shokouhimehr M, Effect of fuels on nanostructure and luminescence properties of combustion synthesized MgAl_2O_4 : Eu^{3+} phosphors, *Journal of Molecular Structure.* 2019; 1193: 274-279.
- [5] Rafiaei S.M, Karimzadeh E, Khodaei M, Ashrafi F, Improved optical properties of Dy^{3+} doped phosphors by spherical SiO_2 particles *Ceramics International.* 2019; 45: 21725-21734.
- [6] Rafiaei S.M, Dini G, Bahrami A, Synthesis, Crystal Structure, Optical and Adsorption Properties of BaAl_2O_4 : Eu^{2+} , $\text{Eu}^{2+}/\text{L}^{3+}$ (L= Dy, Er, Sm, Gd, Nd, and Pr) Phosphors, *Journal of Ceramics International.* 2020; 46: 20243-20250.
- [7] Habibi M.K, Rafiaei S.M, Alhaji A, Zare M, ZnAl_2O_4 : Ce^{3+} phosphors: Study of Crystal Structure, Microstructure, Photoluminescence Properties and Efficient Adsorption of Congo Red Dye, *Journal of Molecular Structure.* 2021; 1228: 129769.
- [8] Ghosh S, Mukherjee S, Banerjee S, Solution Combustion Synthesis of Alumina Spinel and its Characterization. *Int. Ceram. Rev.* 2018; 67: 34-41.
- [9] Spear K.E, Thermodynamic Analysis of Alumina Refractory Corrosion by Sodium or Potassium Hydroxide in Glass Melting Furnaces, 2002 *J. Electrochem. Soc.* 149 B551.
- [10] Tahmasebi K, Paydar M.H, the effect of starch addition on solution combustion synthesis of Al_2O_3 - ZrO_2 nanocomposite powder using urea as fuel, *Materials Chemistry and Physics.* 2008; 109: 156-163.
- [11] Monteiro M.A.F, Photoluminescence behavior of Eu^{3+} ion doped into c- and a-alumina systems prepared by combustion, ceramic and Pechini methods, *Microporous and Mesoporous Materials.* 2008; 108: 237-246.
- [12] Wang J, Zhao D, Zhou G, Zhang C, Zhang P, Hou X, Synthesis of nano-sized c- Al_2O_3 with controllable size by simple, homogeneous precipitation method, *Materials Letters.* 2020; 279: 128476.
- [13] Özdemir H, Faruk Öksüzömer M.A, Synthesis of Al_2O_3 , MgO and MgAl_2O_4 by solution combustion method and investigation of performances in partial oxidation of methane, *Powder Technology.* 2020; 359: 107-117.
- [14] Siva V, Murugan A, Shameem A, Thangarasu S, Kannan S, Raja A, Gel combustion synthesized NiMoO_4 anchored polymer nanocomposites as a flexible electrode material for solid state asymmetric supercapacitors, *International Journal of Hydrogen Energy.* 2023; 48: 18856-18870.
- [15] Sowbhagya N, Harshitha M, Umesha B, Facile one-pot combustion synthesis of CuCo_2S_4 binary nanocomposite for synergetic photodegradation of CR dye and reduction of nitroarenes, *Materials Science and Engineering: B.* 2024; 299: 116992.
- [16] Chen Z, Kang W, Li B, Zhang Q, Hu X, Ding Y, Liang S, Preparation of Mo-Cu composite powder with high homogeneity by solution combustion synthesis, *Journal of Materials Research and Technology.* 2023; 24: 715-723.
- [17] Sarikci S, Topaksu M, Ozturk E, Souadi G, Madkhali O, Madkhali A.Y, Can N, Europium-doped strontium gadolinium oxide phosphor: Investigating structural and photoluminescence characteristics via Sol-Gel combustion synthesis, *Applied Radiation and Isotopes.* 2024; 205: 111169.
- [18] Esmailnejad-Ahranjani P, Lotfi M, Surfactant-assisted combustion synthesis of agglomerated-free, size- and shape-controlled magnetic iron oxide nanoparticles for biomedical applications, *Ceramics International.* 2023; 49: 25113-25120.

[19] Ebrahimi P, Kumar A, Khraisheh M, Combustion synthesis of lanthanum oxide supported Cu, Ni, and CuNi nanoparticles for CO₂ conversion reaction, International Journal of Hydrogen Energy. 2023; 48: 24580-24593.

[20] Roach J.M, Manukyan K.r.V, Dede S, Burns P.C, Aprahamian A, Combustion synthesis of Eu₂O₃ nanomaterials with tunable phase composition and morphology, Journal of Solid State Chemistry .2023; 326: 124235.